JACS
JOURNAL OF THE AMERICAN CHEMICAL SOCIETY

ARTICLE

pubs.acs.org/JACS

Importance of Sialic Acid Residues Illuminated by Live Animal Imaging Using Phosphorylcholine Self-Assembled Monolayer-Coated Quantum Dots

Tatsuya Ohyanagi,[†] Noriko Nagahori,[†] Ken Shimawaki,[†] Hiroshi Hinou,[†] Tadashi Yamashita,[†] Akira Sasaki,[†] Takashi Jin,[‡] Toshihiko Iwanaga,[§] Masataka Kinjo,[†] and Shin-Ichiro Nishimura[†]

[†]Field of Drug Discovery Research, Faculty of Advanced Life Science, Hokkaido University, Sapporo, 001-0021, Japan

[‡]WPI Immunology Frontier Research Center, Osaka University, Yamada-oka 1-3, Suita, Osaka 565-0871, Japan

[§]Department of Anatomy, Hokkaido University Graduate School of Medicine, Sapporo, 060-8638, Japan

Supporting Information

ABSTRACT: Glycans are expected to be one of the potential signal molecules for controlling drug targeting/delivery or long-term circulation of biopharmaceuticals. However, the effect of the carbohydrates of artificially glycosylated derivatives on in vivo dynamic distribution profiles after intravenous injection of model animals remains unclear due to the lack of standardized methodology and a suitable platform. We report herein an efficient and versatile method for the preparation of multifunctional quantum dots (QDs) displaying common synthetic glycosides with excellent solubility and long-term stability in aqueous solution without loss of quantum yields. Combined use of an aminooxy-terminated thiol derivative, 11,11′-dithio bis[undec-11-yl 12-(aminooxyacetyl)amino hexa(ethyleneglycol)], and a phosphorylcholine derivative, 11-mercaptoundecylphosphorylcholine, provided QDs with novel functions for the chemical ligation of ketone-functionalized compounds and the prevention of nonspecific protein adsorption concurrently. In vivo near-infrared (NIR) fluorescence imaging of phosphorylcholine self-assembled monolayer (SAM)-coated QDs displaying various simple sugars (glyco-PC-QDs) after administration into the tail vein of the mouse revealed that distinct long-term delocalization over 2 h can be achieved in cases of QDs modified with α-sialic acid residue (Neu5Ac-PC-QDs) and control PC-QDs, while QDs bearing other common sugars, such as α-glucose (Glc-PC-QDs), α-mannose (Man-PC-QDs), α-fucose (Fuc-PC-QDs), lactose (Lac-PC-QDs), β-glucuronic acid (GlcA-PC-QDs), *N*-acetyl-β-D-glucosamine (GlcNAc-PC-QDs), and *N*-acetyl-β-D-galactosamine (GalNAc-PC-QDs) residues, accumulated rapidly (5−10 min) in the liver. Sequential enzymatic modifications of GlcNAc-PC-QDs gave Galβ1,4GlcNAc-PC-QDs (LacNAc-PC-QDs), Galβ1,4(Fucα1,3)GlcNAc-PC-QDs (Le^x-PC-QDs), Neu5Acα2,3Galβ1,4GlcNAc-PC-QDs (sialyl LacNAc-PC-QDs), and Neu5Acα2,3Galβ1,4(Fucα1,3)-GlcNAc-PC-QDs (sialyl Le^x-PC-QDs) in quantitative yield as monitored by direct matrix-assisted laser desorption ionization time-of-flight mass spectrometry analyses. Live animal imaging uncovered for the first time that Le^x-PC-QDs also distributed rapidly in the liver after intravenous injection and almost quenched over 1 h in similar profiles to those of LacNAc-PC-QDs and Lac-PC-QDs. On the other hand, sialyl LacNAc-PC-QDs and sialyl Le^x-PC-QDs were still retained stably in the whole body after 2 h, while they showed significantly different in vivo dynamics in the tissue distribution, suggesting that structure/sequence of the neighboring sugar residues in the individual sialyl oligosaccharides might influence the final organ-specific distribution. The present results clearly visualize the evidence of an essential role of the terminal sialic acid residue(s) for achieving prolonged in vivo lifetime and biodistribution of various glyco-PC-QDs as a novel class of functional platforms for nanomaterial-based drug targeting/delivery. A standardized protocol using multifunctional PC-QDs should facilitate live animal imaging of ligand-displayed QDs using versatile NIR fluorescence photometry without influence of size-dependent accumulation/excretion pathway for nanoparticles (e.g., viruses) >10 nm in hydrodynamic diameter by the liver.

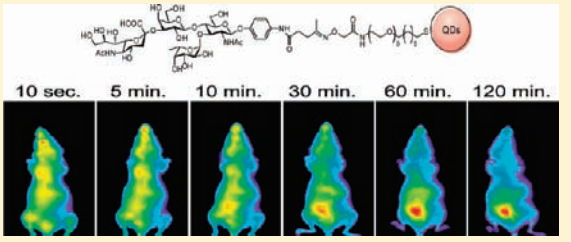

INTRODUCTION

Recent successful approaches of noninvasive imaging for probing in vivo dynamics of glycans and glycoconjugates have provided valuable information on tissue distribution of individual glycosylated compounds, such as small molecular glycans, natural and neoglycoproteins, sugar-modified liposomes, and magnetite-based nanoparticles having glycans.[1] For example, Davis et al. developed for the first time a protocol for the construction of magnetic resonance imaging (MRI)-visible high Fe-content glyconanoparticles having E-/P-selectin ligand carbohydrate that allows presymptomatic in vivo imaging of rat brain disease

Received: December 23, 2010
Published: July 08, 2011

dx.doi.org/10.1021/ja111201c | *J. Am. Chem. Soc.* 2011, 133, 12507–12517

models.[1c] Fukase et al. also reported an efficient method for the synthesis of glycoclusters labeled by ^{68}Ga-1,4,7,10-tetraazacyclododecane-1,4,7,10-tetraacetic acid (^{68}Ga-DOTA) and showed that the use of ^{68}Ga-DOTA labeling of dendrimer-type *N*-glycoclusters made noninvasive imaging of the in vivo dynamics and organ-specific accumulation of various *N*-glycans by positron emission tomography (PET) possible.[1f] It is believed that accumulation of such important data sets of the dynamic biodistribution profiles for individual glycosylated derivatives would become beneficial for further drug discovery research as well as the development of highly sensitive diagnostic methodology based on MRI and PET.

Our attention is now directed toward the influence of scaffold materials to the in vivo dynamics and organ-specific accumulation of the attached glycans. It should be noted that evaluating the effect of carbohydrate moiety of various natural/non-natural glycoconjugates on biodistribution and its lifetime appears to be difficult, independent from the influence by the structure/property of aglycon (nonglycan) moieties, notably artificial scaffold materials, and hydrophobic photosensitive probes as well as protein core structures in native glycoproteins. It is well-known that glycans usually exhibit relatively weak affinity with their partner molecules, such as enzymes and cell surface receptors, even though specificity of the interaction may be very high.[2] To investigate the functional role of carbohydrate itself for controlling glycoprotein circulation and distribution in vivo, it seems likely that a novel class of simple glycoprotein model, in which aglycon-scaffold should entail general globular protein-like structure/property and the potential to prevent nonspecific interaction with other biomolecules, cells, tissues, or artificial materials surfaces, would be used.

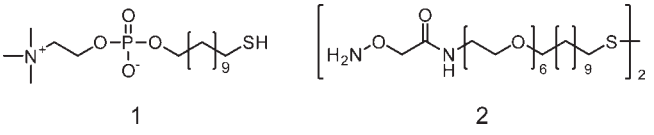

Figure 1. Chemical structures of phosphorylcholine-type monothiol ligand (**1**) and aminooxy-functionalized monothiol anchor group (**2**).

Gold nanoparticles carrying carbohydrates are one of the simplest and most versatile glycoprotein models for probing and investigating functional roles of glycans in vitro using atomic force microscopy (AFM), transmission electron microscopy (TEM), or surface plasmon resonance (SPR).[3] Since it has been documented by in vivo imaging that gold nanoparticles exhibit a higher adsorption than iodine as a X-ray contrast agent with less bone and tissue interference, achieving better contrast with lower X-ray dose,[4] noninvasive imaging of the biodistribution of glycan-conjugated gold nanoparticles may become possible in the near future. On the other hand, quantum dots (QDs) are fluorescence semiconductor nanoparticles that have unique optical properties, including narrow band and size-dependent luminescence with broad absorption, long-term photo stability, and resistance to photobleaching.[5] An attractive application of QDs is the living cells/animals imaging by

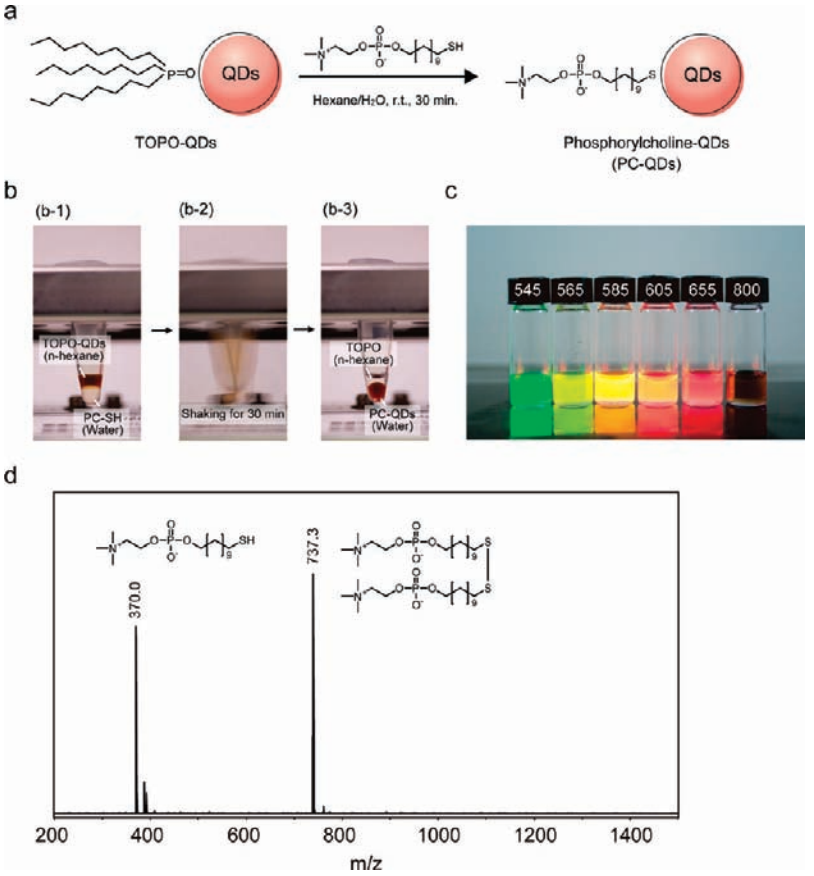

Figure 2. Preparation and characterization of PC-QDs. (a) General protocol of the ligand exchange reaction from TOPO-QDs to PC-QDs. (b) The progress of the ligand exchange reaction: PC-QDs were dissolved in water phase after the ligand exchanging. (c) Photograph of PC-QDs of various emission wavelengths. (d) Direct MALDI-TOFMS analysis of PC-QDs (SeTe/CdS, λ_{em} = 800 nm).

dx.doi.org/10.1021/ja111201c |*J. Am. Chem. Soc.* 2011, 133, 12507–12517

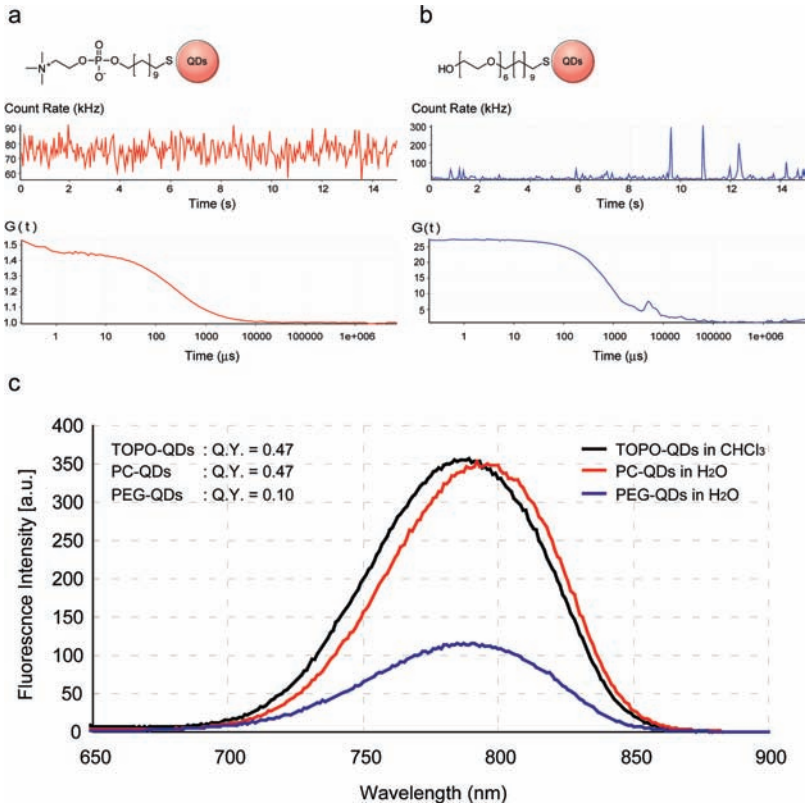

Figure 3. Characterization of PC-QDs and PEG-QDs by FCS. Fluorescence fluctuations of (a) PC-QDs and (b) PEG-QDs in water. The autocorrelation curves were fitted by using one component diffusion model. (c) Fluorescence spectra of QDs coated by TOPO in chloroform, PC-SH, and PEG-SH[17] in water. The fluorescence spectra were measured by using an excitation at 488 nm, and the quantum yield was estimated by absolute photoluminescence quantum yield measurement. PEG-QDs were prepared by the same procedure for the preparation of PC-QDs using PEG-SH[17] instead of PC-SH.

simple fluorescent measurements,[6] which is possible due to successful surface modifications with various biomolecules, such as DNA,[7] peptides,[8] proteins,[9] antibodies,[10] and carbohydrates.[11] As a scaffold to display carbohydrates and investigate their functions, advantages of QDs are summarized as follows: (a) QDs can be detected and monitored in vivo by simple fluorescent photometric analysis without any special and expensive equipment. (b) Multiple carbohydrates can be displayed on a single QD, and the carbohydrate density on the single QD can be readily controlled. Thus enhanced affinity with target molecules is expected as a result of the glycoside cluster effect.[2] (c) The QDs range in size from several and to dozens of nanometers, the same level as typical folded proteins (~10 nm in diameter),[3c] is suitable for designing a new class of glycoprotein models. It is therefore expected that the QDs will exhibit behavior and dynamics similar to common globular proteins distributed in living cells and animals.[6e,i] Since inorganic, metal-containing QDs are generally synthesized in organic solvents by coating with hydrophobic ligands, such as trioctylphosphine oxide (TOPO),[5,6] it is obvious that surface modification of QDs is needed to improve solubility and stability in common physiological conditions. Thus far, many water-soluble QDs have been developed by coating with a variety of thiols and copolymers based on poly(ethylene glycols) (PEG)-like structures.[6e] Recently, Seeberger et al. developed a convenient method to prepare different sugar-capped PEGylated QDs that can be used for in vitro imaging and in vivo liver targeting, in which paraffin sections of mouse livers were prepared for the visualization of QDs by fluorescence microscopy.[1e] However, it should be noted that the nanoparticle hydrodynamic diameter is a crucial design parameter in the development of potential diagnostic and therapeutic agents. Organic coatings often result in a significant increase of the final hydrodynamic diameter. In fact, QDs > 10 nm in hydrodynamic diameter were proved to be accumulated by the liver designed specifically to capture and eliminate nanoparticles, while smaller QDs < 5.5 nm resulted in rapid renal excretion.[6i] There is no versatile QDs platform mimicking typical folded proteins (~10 nm in diameter) to have satisfactory functions for both displaying glycans and reducing nonspecific interactions with abundant serum and cellular proteins without loss of quantum yield of the original QDs. Here we communicate a standardized protocol for the construction of an ideal glycoprotein model, namely phosphorylcholine self-assembled monolayers (SAMs)[12]-coated QDs displaying various glycans (glyco-PC-QDs), exhibiting excellent water solubility, long-term stability in the stock solution, pH resistance, and a capacity to prevent nonspecific protein adsorption.

RESULTS AND DISCUSSION

QDs Coated by Phosphorylcholine SAMs. It is well-known that surface modification by thiol tethering or copolymers containing PEG-like structures is one of the most commonly used methods for the solubilization of QDs.[5,6] However, we thought that the use of phospholipid-like derivatives is a potential alternative to PEGylation because phosphatidylcholine is the most abundant and indispensable lipid component of stable biomembranes. We hypothesized that combined use of a simple monothiol, 11-mercaptoundecylphosphorylcholine (PC-SH, **1**),[12c] and an aminooxy-terminated thiol

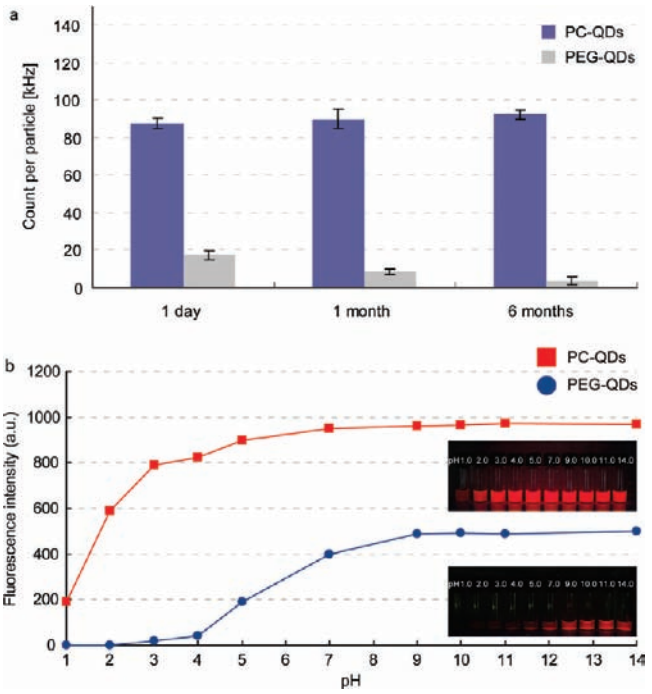

Figure 4. Long-term stability and pH resistance. (a) Fluorescence intensity per molecule was measured and estimated by FCS for the solutions of PC-QDs and PEG-QDs stored in water at 4 °C in the dark for 6 months. (b) The fluorescence intensity measured by spectrophotometer and photograph under UV irradiation at 365 nm of PC-QDs and PEG-QDs in aqueous buffer solutions at various pHs.

derivative, 11,11′-dithio bis[undec-11-yl 12-(aminooxyacetyl)amino hexa(ethyleneglycol)] (ao-SH, **2**),[13] should provide QDs with promising characteristics, such as much higher solubility, stability, and ability to display multiple ligands as well as biomembrane-mimetic surface properties (Figure 1). Jiang et al. revealed that zwitterions with a balanced charge and minimized dipole are crucial for the strong resistance of phosphorylcholine SAMs formed on a gold-coated chip to protein adsorption due to their strong hydration capacity through electrostatic interaction.[12c] Phosphorylcholine SAMs on magnetic beads[12d] could also be applied for stable supporting materials to immobilize reusable engineered glycosyltransferases. In addition, our previous study demonstrated that simple glycans and glycosphingolipid derivatives enriched by glycoblotting reaction with ao-SH (**2**) on gold nanoparticles can be directly ionized from Au surfaces under general matrix-assisted laser desorption ionization (MALDI) condition.[13,14] Taking the characteristics of the two monothiol derivatives **1** and **2** into account, the present protocol seems to be advantageous for the construction of a variety of compound library displayed on the QD surfaces in a controlled density because the structure (quality) and the quantity of molecules displayed on QDs might be determined concurrently by direct matrix-assisted laser desorption ionization time-of-flight mass spectrometry (MALDI-TOFMS) without any purification or pretreatment procedure.

To assess the feasibility of PC-SH (**1**) as a novel coating material for improving the properties of QDs surface, various PC-QDs were prepared by ligand exchange reaction of PC-SH with TOPO-coated QDs (Figure 2a). Reaction of compound **1** with commercially available TOPO-coated QDs with diameters in a range from 5.8 to 9.3 nm (CdSe/ZnS, λ_{em} = 545, 565, 585, 605, and 655 nm) and synthetic TOPO-coated QDs of 11.7 nm (CdSeTe/CdS, λ_{em} = 800 nm)[15] proceeded smoothly and gave PC-QDs showing excellent solubility toward water (Figure 2b and c). The surface modification with PC-SH (**1**) was directly confirmed by MALDI-TOFMS (Figure 2d), where the peaks at m/z 370.0 and 737.3 are simply assigned as PC-SH and disulfide form (PC−S−S−PC). Solubility toward water and the fluorescence intensity of PC-QDs was evaluated by fluorescence correlation spectroscopy (FCS)[15,16] in comparison with those of simple PEG-QDs. As shown in Figure 3, the fluorescence fluctuation of PC-QDs was proved to be rapid and an ideal profile in the fitting curves with single-component diffusion model (Figure 3a), suggesting that PC-QDs are well dispersed in water, while the results of PEG-QDs showed an evidence of the formation of serious aggregation shortly after PEGylation of QDs surface (Figure 3b). The diffusion coefficient and the hydrodynamic diameter of PC-QDs prepared from SeTe/CdS-type QDs were estimated to be 18.2 $\mu m^2\ s^{-1}$ and 11.7 ± 1.5 nm, based on the value of diffusion coefficient using 20 nm when fluospheres fluorescent beads (D = 10.4 $\mu m^2\ s^{-1}$) were used as a standard material. On the contrary, PEG-QDs did not show any satisfactory fitting profile with neither the one- nor the two-component diffusion model, suggesting the importance of amphoteric nature of the PC-QDs for preventing aggregation of QDs capped with monothiol derivatives. It was also revealed by absolute photoluminescence quantum yield measurement that quantum yield of PC-QDs in water is identical to that of TOPO-QDs in $CHCl_3$ (quantum yield = 0.47), while the quantum yield of PEG-QDs in H_2O was reduced to be 0.1 after PEG-SH [(1-mercaptoundec-11-yl)hexa(ethylene glycol)][17] coating (Figure 3c). Given the facts that the quantum yields of QDs generally appear to decrease by the ligand exchange reaction with general thiol compounds,[10b,18] long-alkyl monothiol derivatives having both amphoteric and amphipathic properties might be essential to retain high fluorescence quantum yields and to prevent aggregation due to nonspecific interactions. It was reported that QDs capped by zwitterionic ligands, such as cysteine (Cys)[6h] and dihydrolipoic acid modified by sulfobetaine (DHLA-SB),[6l] preserved QD optical properties and excellent stability as well as good resistance to pH variations, while Cys-QDs quickly aggregated after a few days.

Merit of the use of compound **1** is evident because PC-QDs showed prominently long-term stability in water at 4 °C and excellent resistance to an extensive range of pH (pH 2−14) as compared with those of PEG-QDs (Figure 4a and b). Surprisingly, PC-QDs were stable for at least 6 months, and the loss of fluorescence intensity was only 20% even at pH of 3. These favorable characteristics of PC-QDs are quite similar to those observed for DHLA-SB-QDs capped by a dithiol anchor group.[6l] This suggests clearly that a balanced charge of zwitterions and a minimized dipole of monothiol **1** are essential for the strong resistance of phosphorylcholine SAMs formed on QDs from aggregation due to their strong hydration capacity through electrostatic interaction.[12c] Moreover, it was also demonstrated that monothiol anchor can stabilize QDs surface efficiently when such suitable amphoteric nature was incorporated into the hydrophilic head as well as good molecular packing of the hydrophobic linker moiety.

Construction of Glyco-PC-QDs as Glycoprotein Models. General glycans released from naturally occurring glycoconjugates such as *N*- and *O*-glycans of glycoproteins and glycosphingolipid derivatives with oligosaccharide head groups can be directly captured by "glycoblotting",[19] a promising method for

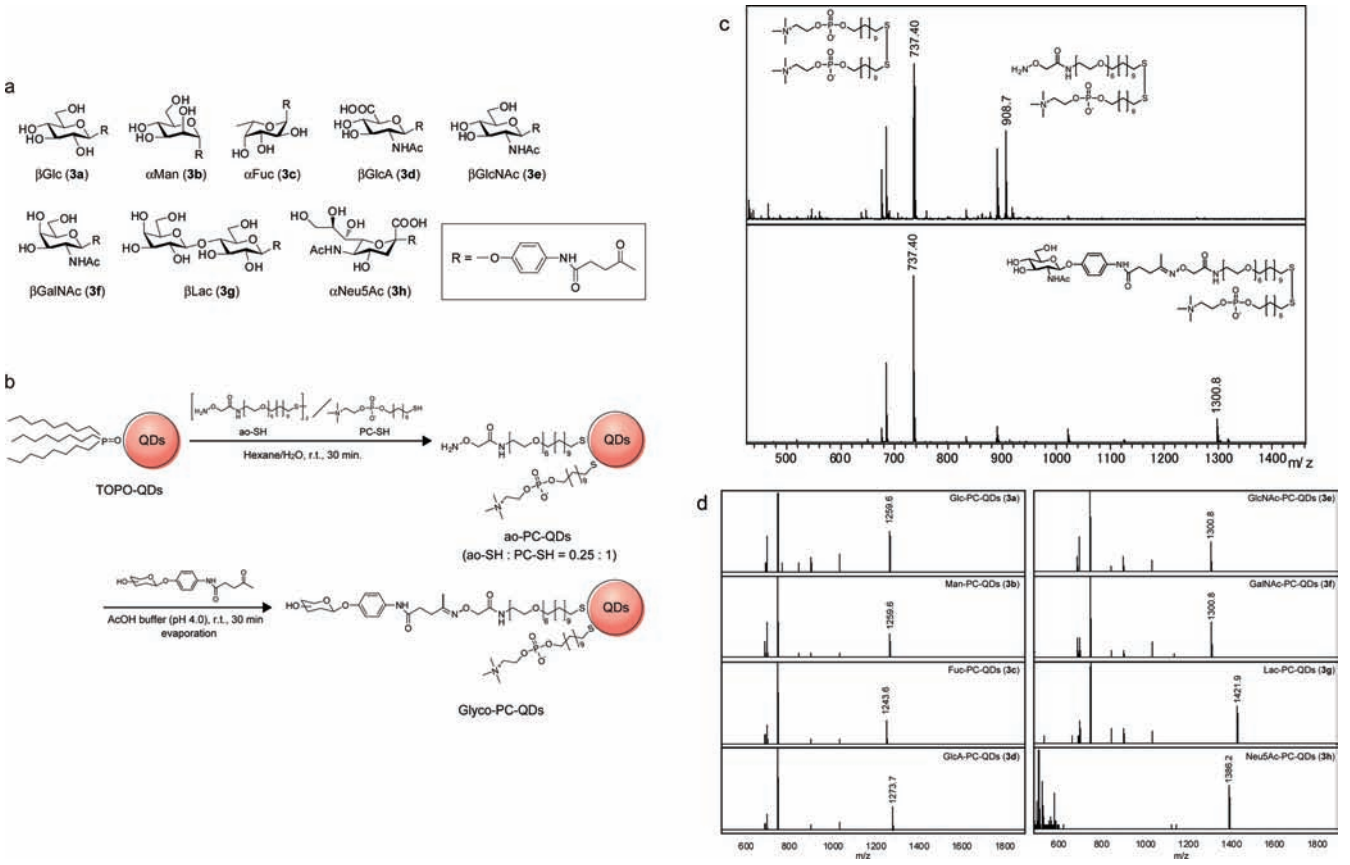

Figure 5. The preparation of glyco-PC-QDs. (a) chemical structures of *p*-(4-oxopentanamido)-phenyl glycosides **3a**—**h**. (b) A simple protocol for the preparation of glyco-PC-QDs by the reaction of ao-PC-QDs with glycosides **3a**—**h**. (c) Glycoblotting of **3a** by ao-PC-QDs monitored by MALDI-TOFMS. (d) MALDI-TOFMS of various glyco-PC-QDs. MALDI-TOFMS were measured at positive mode, while Neu5Ac-PC-QDs needed negative mode due to carboxyl groups.

chemoselective ligation of any reducing sugars or compounds bearing aldehyde/ketone by use of the aminooxy/hydrazide-functionalized materials.[13,19] To display general carbohydrates and synthetic glycosides efficiently on the surface of QDs in combination with phosphorylcholine SAMs, we selected an aminooxy-functionalized ao-SH (**2**)[13] containing 11-mercaptoundecyl moiety, an alkanethiol anchor group of PC-SH (**1**), in order to obtain an appropriate molecular packing structure of SAMs on QDs. As expected, QDs surface could be coated efficiently by the mixed SAMs of ao-SH (**2**) and PC-SH (**1**) at an arbitrary ratio and afforded a novel class of multifunctional QDs (ao-PC-QDs) as characterized by direct MALDI-TOFMS and FCS.

Glycoblotting of free sugars by the aminooxy-functional group induces generally ring-opening reaction at the reducing end of any carbohydrates and gives a mixture of *E*/*Z*-isomers during stable oxime bond formation.[19] To control the stereochemistry at an anomeric carbon of the reducing end of oligosaccharides even in cases of simple monosaccharides, we decided to employ versatile *p*-nitrophenyl glycosides as key starting materials. Various *p*-nitrophenyl glycosides readily prepared by conventional synthetic methods were converted into *p*-(4-oxopentanamido)-phenyl glycosides **3a**—**h** in high yields (Figure 5a and Scheme S1, Supporting Information). Reactions of glycosides **3a**—**h** with ao-PC-QDs (ao-SH/PC-SH = 2/8) proceeded smoothly in acetic acid buffer (pH of 4.0) for 30 min at room temperature to afford glyco-PC-QDs carrying β-Glc (Glc-PC-QDs), α-Man (Man-PC-QDs), α-Fuc (Fuc-PC-QDs), β-GlcA (GlcA-PC-QDs), β-GlcNAc (GlcNAc-PC-QDs), β-GalNAc (GalNAc-PC-QDs), β-Lac (Lac-PC-QDs), and α-Neu5Ac (Neu5Ac-PC-QDs), respectively (Figure 5b). As shown in Figure 5c, the signal at *m*/*z* 908.7 corresponding to ao—S—S—PC disappeared completely instead of the advent of new signal at *m*/*z* 1259.6 due to a heterodisulfide bearing Glc residue, indicating successful oxime bond formation between ao-PC-QDs and ketone-functionalized glycoside **3a**. Similarly, all other products derived by the reactions of **3b**—**h** with ao-PC-QDs were also characterized as signals corresponding to the heterodisulfides by MALDI-TOFMS (Figure 5d). As shown in Figure 6, the GlcNAc residues on the GlcNAc-PC-QDs were quantified simply by measuring ^{1}H NMR spectrum of QDs directly. No unreacted aminooxy functional group ($H_2N—O—CH_2—$ at 4.17 ppm) was detected after glycoblotting with compound **3e** (Figure 6b), and the product generated by treating the GlcNAc-PC-QDs with I_2 was also fully characterized as the reasonable composition (Figure 6c). These results clearly indicate that the ratio of glycan/PC on the QD surface can be controlled by that of ao-SH/PC-SH of the ao-PC-QDs. As indicated by the TEM views in Figure 6d and e, the diameters of ao-PC-QDs and GlcNAc-PC-QDs were proved to be a range from 7 nm (short side) to10 nm (long side), and the results were in good agreement with those estimated by FCS (~11 nm).

In our previous study,[14] it was demonstrated that simple sugar residues displayed on the surface of gold nanoparticles (3—8 nm in diameter) can be further modified by some glycosyltransferases in the presence of sugar nucleotides. Here we examined

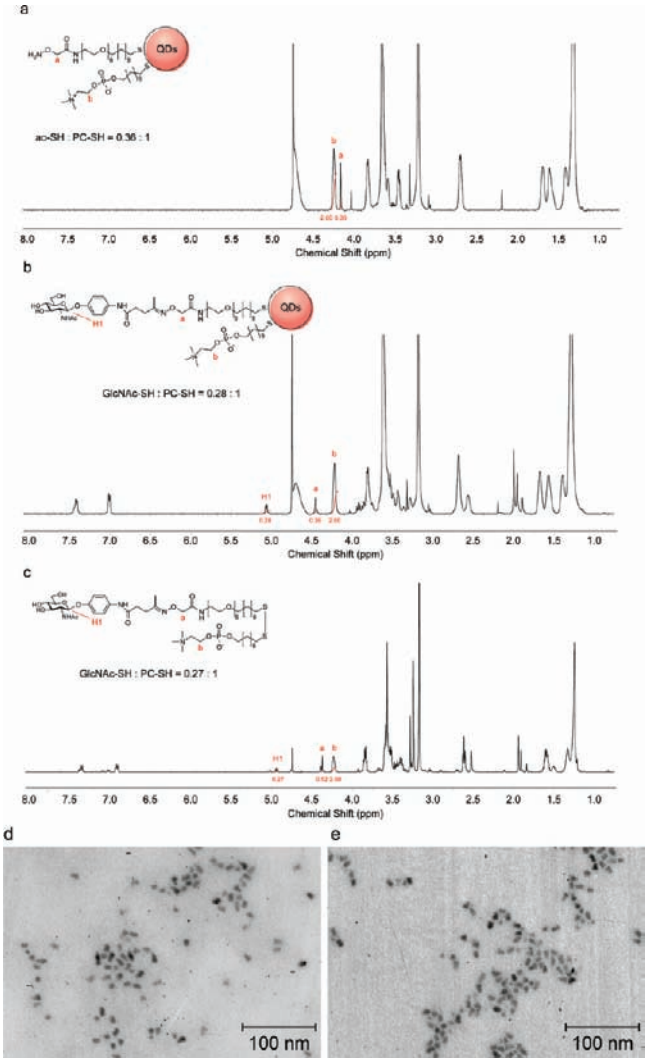

Figure 6. Characterization of Glyco-PC-QDs by ^{1}H NMR and TEM. (a) ao-PC-QDs, (b) GlcNAc-PC-QDs, (c) the product generated by treating GlcNAc-PC-QDs with I_2. TEM views of (d) ao-PC-QDs and (e) GlcNAc-PC-QDs. See also Supporting Information.

the conversion of a simple glyco-PC-QDs (**3c**) into more complicated glyco-PC-QDs bearing LacNAc (**4**), Le^x (**5**), sialyl LacNAc (**6**), and sialyl Le^x (**7**) by treating with recombinant β1,4GalT, α1,3FucT, and α2,3Neu5Ac in the presence of suited sugar nucleotides under a general condition of enzymatic synthesis[20] (Figure 7a). Surprisingly, all reactions proceeded smoothly and afforded target derivatives in quantitative yields, respectively, as monitored by MALDI-TOFMS shown in Figure 7b. Given the fact that globular protein-like dendrimers having spherical molecular shape and size (~10 nm in diameter) are ideal polymer supports in the fully automated enzymatic glycan synthesis,[20d] glyco-PC-QDs **3c** and **4**−**6** appear to become a convenient glycoprotein-like model. These results clearly indicate that a strategy based on enzymatic sugar elongation of chemically synthesized simple glyco-PC-QDs allows for the construction of highly complicated glycan-conjugated PC-QDs library.

As indicated in Figure 7c, ao-PC-QDs, GlcNAc-PC-QDs (**3c**), and sialyl Le^x-PC-QDs (**7**) exhibited good fitting curves with a single-component diffusion model of the FCS analyses, suggesting that the excellent dispersibility and fluorescence property of PC-QDs/ao-PC-QDs were not changed during sugar elongation reactions of GlcNAc-PC-QDs (**3c**) by sequential treatment with three glycosyltransferases.

Live Animal NIR Fluorescence Imaging by Means of Glyco-PC-QDs. Glyco-PC-QDs (CdSeTe/CdS) derived from NIR ao-PC-QDs with an excitation of 710 nm and an emission of 800 nm were employed for live animal imaging in order to reduce nonspecific photoabsorption by biomolecules.[15,21] Initially, we tested the real-time fluorescent monitoring of Lac-PC-QDs (**3g**) and Neu5Ac-PC-QDs (**3h**) in comparison with PC-QDs as a control after injection into the vein of mouse tail (Figure 8a). Choi et al. reported that QDs of 5.5 nm or less drained from urine immediately and that those of 5.5 nm or more accumulated in the liver,[6i] even though cysteine[6h] was employed as a zwitterionic component in addition to DHLA, cysteamine, and DHLA-PEG. Therefore, it seemed that PC-QDs may distribute in the liver according to this size effect of QDs, since NIR PC-QDs with ca. 11.7 nm in diameter were tested for the present live animal imaging. In addition, it was also considered that Lac-PC-QDs should accumulate in the liver quickly due to the hepatic asialoglycoprotein receptor[22] responsible for the specific interaction with terminal β-Gal residues of various oligosaccharides, while Neu5Ac-PC-QDs might show a different organ distribution profile due to the effect of sialic acids. As anticipated, it was demonstrated that QDs bearing lactose **3g** began to accumulate in the liver immediately after administration. However, PC-QDs and Neu5Ac-PC-QDs did not distribute in any specific organ, indicating that nonfouling behavior observed in PC-QDs is due to the different mechanism from the resistance to nonspecific protein adsorption by QDs displaying cysteine[6h] having amino and carboxyl groups. Highly packing structure of monothiol phosphorylcholine-SAMs may provide QDs surface with specific nonfouling nature by strong hydration capacity through electrostatic interaction. This characteristic of PC-QDs was not influenced by modification with Neu5Ac residues, while lactose moiety in Lac-PC-QDs (**3g**) drastically altered PC-QDs as liver-directed QDs. Interestingly, a photograph taken 10 min after the injection of other glyco-PC-QDs (**3a**−**f**) revealed that PC-QDs having Glc, Man, Fuc, GlcNAc, and GalNAc also accumulated immediately in the liver, while GlcA-PC-QDs (**3d**) did not (Figure 8b). Surgery confirmed that the entire liver strongly fluoresced with Glc-PC-QDs and GlcNAc-PC-QDs, and the bottom edge of the liver weakly fluoresced with GlcA-PC-QDs (data not shown). These results clearly showed that distinct long-term delocalization over 2 h is observed only in cases of QDs modified with α-sialic acid (Neu5Ac-PC-QDs) and control PC-QDs, while QDs bearing other popular neutral sugars were accumulated rapidly (5−10 min) in the liver. This trend was preliminarily demonstrated by photographs of fluoresced organs isolated from tested mice injected by three typical materials, PC-QDs, Lac-PC-QDs, and Neu5Ac-PC-QDs (Figure 8c). It should also be noted that β-glucuronic acid (GlcA-PC-QDs) appeared to show a different metabolic profile when compared with other glyco-PC-QDs.

Considering that PC-QDs were proved to be an ideal scaffold material mimicking general globular proteins having specific nonfouling surface, our interest was next focused on the insight into functional roles of the terminal sialic acid residues involving in the characteristic oligosaccharide moieties, such as sialyl Lewis antigens known as important core structures for possible ligands of mammalian lectins, such as selectins.[23] In vivo NIR

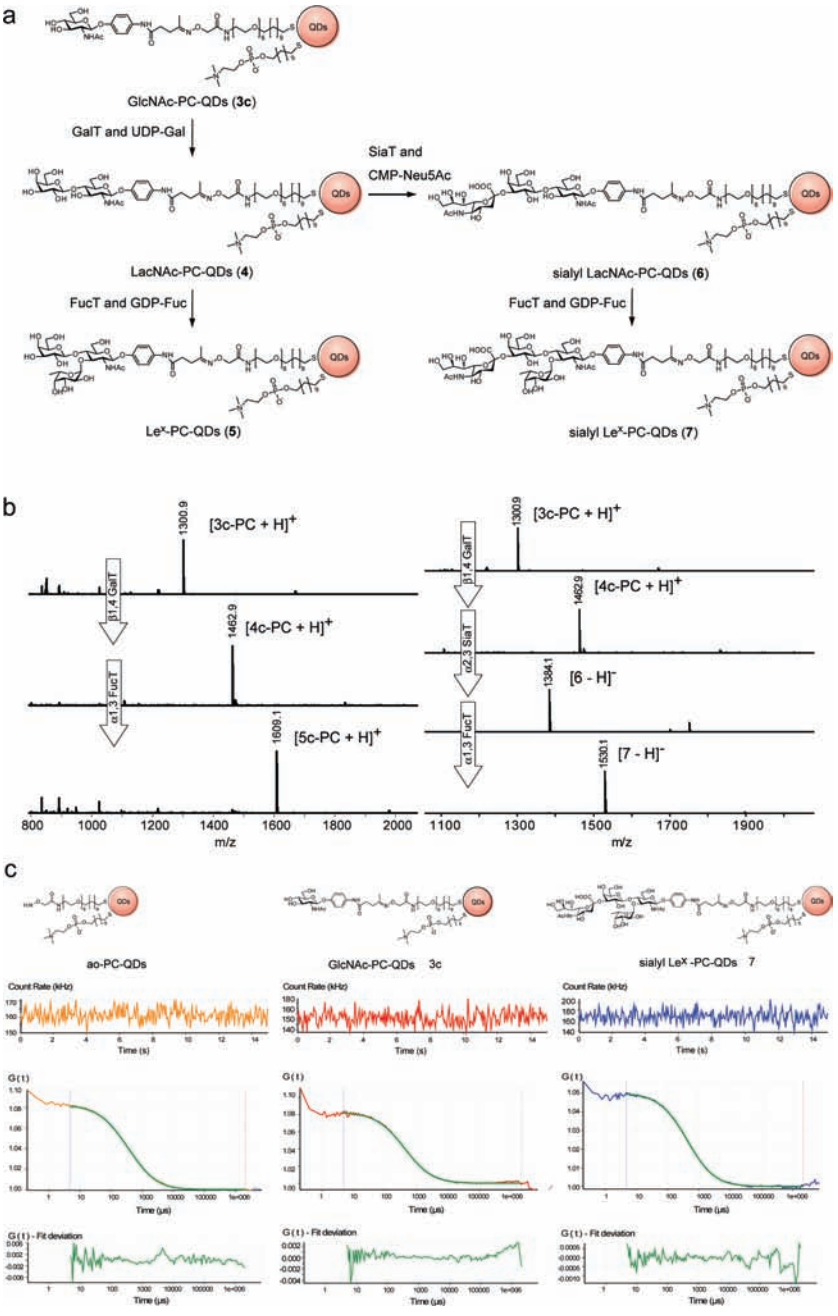

Figure 7. Enzymatic sugar extension of GlcNAc-PC-QDs. (a) Synthetic route of four glyco-PC-QDs by means of three recombinant glycosyltransferases and sugar nucleotides. (b) Monitoring the processes of enzymatic modifications by direct MALDI-TOFMS. (c) Fluorescence fluctuations of ao-PC-QDs, GlcNAc-PC-QDs (**3c**), and sialyl Le^x-PC-QDs (**7**) in water. The autocorrelation curves were fitted by using an one component diffusion model.

fluorescence imaging using PC-QDs displaying LacNAc (**4**), Le^x (**5**), sialyl LacNAc (**6**), and sialyl Le^x (**7**) uncovered for the first time that Le^x-PC-QDs (**5**) are also accumulated rapidly (5−30 min) in the liver after intravenous injection and almost quenched over 1 h in a similar profile to that of LacNAc-PC-QDs (**4**) (Figure 9a). On the other hand, sialyl LacNAc-PC-QDs (**6**) and sialyl Le^x-PC-QDs (**7**) were still retained stably in the body after 2 h while they exhibited significantly different in vivo dynamics in the tissue distribution observed by dissection at 2 h after injection. As indicated in Figure 9b, sialyl LacNAc-PC-QDs (**6**) appeared to locate spleen or intestine, and sialyl Le^x-PC-QDs (**7**) did not localize in any organs, while Le^x-PC-QDs (**5**) distributed specifically in the liver. These results suggest that structure/sequence of the neighboring sugar residues in the individual sialylated oligosaccharides might influence significantly the organ-specific distribution after long-term circulation. Disappearance of fluorescence of these glyco-PC-QDs after administration might be due to the disintegration in the body without any leaking into urinary bladder or the urine. Metabolism and excretion pathway of PC-QDs and individual sialic acid-containing glyco-PC-QDs after injection into mice remains unclear, while there was no significant change in cell viability tested by using A549 cells between PC-QDs and GlcNAc-PC-QDs (Figure S4, Supporting Information).

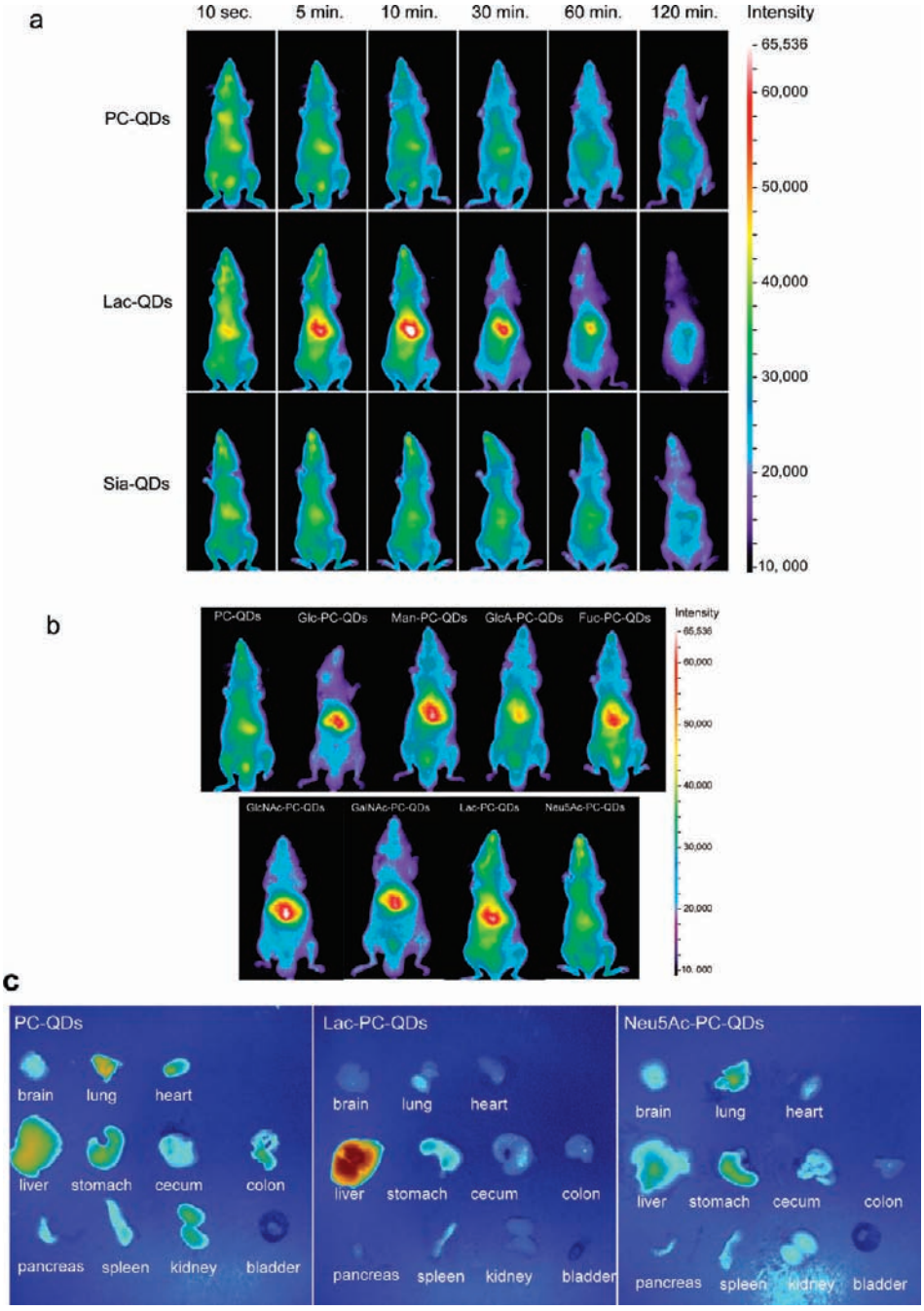

Figure 8. Live animal imaging of glyco-PC-QDs. (a) Imaging of PC-QDs, Lac-PC-QDs (**3g**), and Neu5Ac-PC-QDs (**3h**) after injection of 100 pmole of glyco-PC-QDs. (b) Pictures taken 10 min after administration of QDs carrying **3a**−**h** compared with PC-QDs. The mice were imaged using Lumazone equipped with Photometrics Cascade II EM CCD camera. QDs were excited with 710 nm, and emission filter was 800/12 nm bandpass filter. (c) Photographs of major organs isolated from three tested mice (PC-QDs, Lac-PC-QDs, and Nue5Ac-PC-QDs) at 2 h after administration.

CONCLUSION

We established a standardized procedure for the preparation of PC-QDs, highly sensitive, stable, and nonfouling QDs coated by phosphorylcholine SAMs by means of a simple monothiol, 11-mercaptoundecylphosphorylcholine (PC-SH, **1**). Combined use of **1** with an aminooxy-terminated thiol derivative, 11,11′-dithio bis[undec-11-yl 12-(aminooxyacetyl)amino hexa(ethyleneglycol)] (ao-SH, **2**), allowed for the construction of an ideal glycoprotein model, namely glyco-PC-QDs, through the glycoblotting-based chemical ligation with ketone-functionalized synthetic glycosides. Further enzymatic modifications of simple glyco-PC-QDs provided QDs having more complicated Lewis antigen-related oligosaccharides. It was demonstrated that a nonfouling characteristic of highly stable PC-QDs makes in vivo direct monitoring of glycan-specific interaction and distribution of glyco-PC-QDs after injection into the vein of mouse tail possible. Live animal NIR fluorescence imaging of glyco-PC-QDs revealed the importance of the terminal sialic acid residues for achieving prolonged in vivo lifetime[24] without size-dependent liver localization of nanoparticles.[6i] Advantage of the present approach is clear because

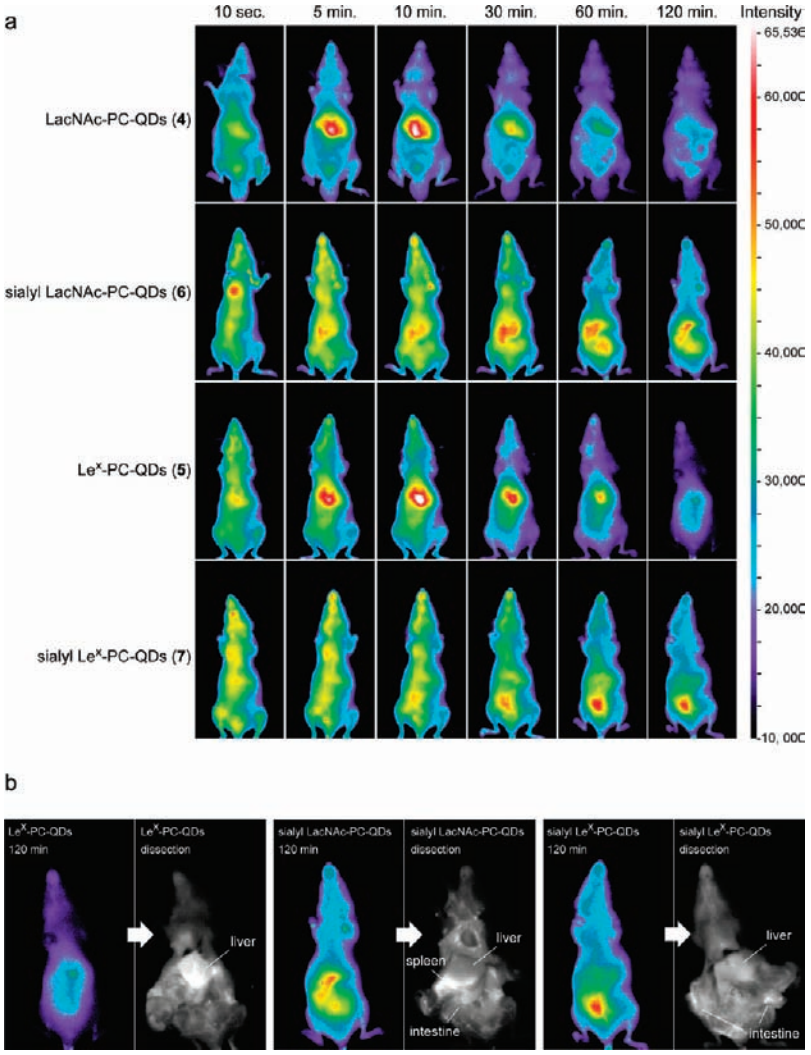

Figure 9. Live animal imaging of glyco-PC-QDs carrying Lewis antigen-related oligosaccharides. (a) Time course after injection of 100 pmole of glyco-PC-QDs (**4**−**7**). (b) Distribution of glyco-PC-QDs carrying Le^x (**5**), sialyl LacNAc (**6**), and sialyl Le^x (**7**) uncovered preliminarily by dissection at 2 h after administration.

ao-PC-QDs are a novel class of convenient and versatile scaffold for displaying a variety of compounds having reactive ketone/aldehyde as well as reducing sugars and synthetic glycosides used in this study. Considering the impact of current and emerging nanomaterials systems for the development of practical drug delivery,[25] the present strategy would enable entirely novel classes of therapeutics.

■ ASSOCIATED CONTENT

Supporting Information. Experimental sections for the preparation of PC-QDs, ao-PC-QDs, glyco-PC-QDs, synthesis of glycosides, structural characterizations by NMR, characterization of QDs, live animal NIR fluorescence imaging, and complete refs 24a and 24d. This material is available free of charge via the Internet at http://pubs.acs.org.

■ AUTHOR INFORMATION

Corresponding Author
shin@glyco.sci.hokudai.ac.jp.

■ ACKNOWLEDGMENT

This work was supported partly by a program "Innovation COE program for future drug discovery and medical care" from the Ministry of Education, Culture, Science, and Technology, Japan.

■ REFERENCES

(1) (a) Laughlin, S. T.; Baskin, J. M.; Amacher, S. L.; Bertozzi, C. R. *Science* **2008**, *320*, 664–667. (b) Andre, S.; Kozar, T.; Kojima, S.; Unverzagt, C.; Gabius, H.-J. *Biol. Chem.* **2009**, *390*, 557–565. (c) Kasteren, S. I.; Campbell, S. J.; Serres, S.; Anthony, D. C.; Sibson, N. R.; Davis, B. G. *Proc. Natl. Acad. Sci. U.S.A.* **2009**, *106*, 18–23. (d) Marradi, M.; Alcantara, D.; de la Fuente, J. M.; Garcia-Martin, M. L.; Cerdan, S.; Penades, S. *Chem. Commun.* **2009**, 3922–3924. (e) Kikkeri, R.; Lepenies, B.; Adibekian, A.; Laurino, P.; Seeberger, P. H. *J. Am. Chem. Soc.* **2009**, *131*, 2110–2112. (f) Tanaka, K.; Siwu, E. R.; Minami, K.; Hasegawa, K.; Nozaki, S.; Kanayama, Y.; Koyama, K.; Chen, W. C.; Paulson, J. C.; Watanabe, Y.; Fukase, K. *Angew. Chem., Int. Ed.* **2010**, *49*, 8195–8200.

(2) (a) Lee, Y. C. *FASEB J.* **1992**, *6*, 3193–3200. (b) Lee, Y. C.; Lee, R. T. *Acc. Chem. Res.* **1995**, *28*, 321–327. (c) Mammen, M.; Choi, S. K.;

Whitesides, G. M. *Angew. Chem., Int. Ed.* **1998**, *37*, 2754–2794. (d) Lundquist, J. J.; Toone, E. J. *Chem. Rev.* **2002**, *102*, 555–578.

(3) (a) de la Fuente, J. M.; Eaton, P.; Barrientos, A. G.; Rojas, T. C.; Rojo, J.; Canada, J.; Fernandez, A.; Penades, S. *Angew. Chem., Int. Ed.* **2001**, *40*, 2257–2261. (b) Katz, E.; Willner, I. *Angew. Chem., Int. Ed.* **2004**, *43*, 6042–6108. (c) Marradi, M.; Martin-Lomas, M.; Penades, S. *Adv. Carbohydr. Chem. Biochem.* **2010**, *64*, 211–290.

(4) Hainfeld, J. F.; Slatkin, D. N.; Focella, T. M.; Smilowitz, H. M. *Br. J. Radiol.* **2006**, *79*, 248–253.

(5) (a) Reed, M. A.; Randall, J. N.; Aggarwal, R. J.; Matyi, R. J.; Moore, T. M.; Wetsel, A. E. *Phys. Rev. Lett.* **1988**, *60*, 535–537. (b) Rossetti, R.; Nakahara, S.; Brus, L. E. *J. Chem. Phys.* **1983**, *79*, 1086–1088. (c) Gleiter, H. *Adv. Mater.* **1992**, *4*, 474–481. (d) Alivisatos, A. P. *Science* **1996**, *271*, 933–937.

(6) (a) Bruchez, M., Jr.; Moronne, M.; Gin, P.; Weiss, S.; Alivisatos, A. P. *Science* **1998**, *281*, 2013–2016. (b) Chan, W. C.; Nie, S. *Science* **1998**, *281*, 2016–2018. (c) Jaiswal, J. K.; Mattoussi, H.; Mauro, J. M.; Simon, M. *Nat. Biotechnol.* **2003**, *21*, 47–51. (d) Gao, X.; Cui, Y.; Levenson, R. M.; Chung, W. K.; Nie, S. *Nat. Biotechnol.* **2004**, *22*, 969–976. (e) Medintz, I. L.; Uyeda, H. T.; Goldman, E. R.; Mattoussi, H. *Nat. Mater.* **2005**, *4*, 435–446. (f) Uyeda, H. T.; Medintz, I. L.; Jaiswal, J. K.; Simon, S. M.; Mattoussi, H. *J. Am. Chem. Soc.* **2005**, *127*, 3870–3878. (g) Michalet, X.; Pinaud, F. F.; Bentolila, L. A.; Tsay, J. M.; Doose, S.; Li, J. J.; Sundaresan, G.; Wu, A. M.; Gambhir, S. S.; Weiss, S. *Science* **2005**, *307*, 538–544. (h) Liu, W.; Choi, H. S.; Zimmer, J. P.; Tanaka, E.; Frangioni, J. V.; Bawendi, M. G. *J. Am. Chem. Soc.* **2007**, *129*, 14530–14531. (i) Choi, H. S.; Liu, W.; Misra, P.; Tanaka, E.; Zimmer, J. P.; Ipe, B. I.; Bawendi, M. G.; Frangioni, J. V. *Nat. Biotechnol.* **2007**, *25*, 1165–1170. (j) Liu, W.; Howarth, M.; Greytak, A. B.; Zheng, Y.; Nocera, D. G.; Ting, A. Y.; Bawendi, M. G. *J. Am. Chem. Soc.* **2008**, *130*, 1274–1284. (k) Liu, W.; Greytak, A. B.; Lee, J.; Wong, C. R.; Park, J.; Marshall, L. F.; Jiang, W.; Curtin, P. N.; Ting, A. Y.; Nocera, D. G.; Fukumura, D.; Jain, R. K.; Bawendi, M. *J. Am. Chem. Soc.* **2010**, *132*, 472–483. (l) Muro, E.; Pons, Lequeux, N.; Fragola, A.; Sanson, N.; Lenkei, Z.; Dubertret, B. *J. Am. Chem. Soc.* **2010**, *132*, 4556–4557.

(7) (a) Dubertret, B.; Skourides, P.; Norris, D.; Noireaux, V.; Brivanlous, A.; Libchaber., A. *Science* **2002**, *298*, 1759–1762. (b) Gill, R.; Willner, I.; Shweky, I.; Banin, U. J. *Phys. Chem. B* **2005**, *109*, 23715–23719.

(8) (a) Cai, W.; Shin., D. W.; Chen, K.; Gheysens., O.; Cao, Qizhen.; Wang, S. W.; Gambhir, S. S.; Chen, X. *Nano lett.* **2006**, *6*, 669–676. (b) Akerman, M.; Chan, W. C.; Laakkonen, P.; Bhatia, S. N.; Ruoslahti, E. *Proc. Natl. Acad. Sci. U.S.A.* **2002**, *99*, 12617–12621.

(9) (a) Mattoussi, H.; Mauro, J. M.; Goldman, E. R.; Anderson, G. P.; Sundar, V. C.; Mikulec, F. V.; Bawendi., M. G. *J. Am. Chem. Soc.* **2000**, *122*, 12142–12150. (b) Clapp, A. R.; Medintz, I. L.; Mauro, J. M.; Fisher, B. R.; Bawendi, M. G.; Mattoussi, H. *J. Am. Chem. Soc.* **2004**, *126*, 301–310. (c) Han, H.-S.; Devaraj, N. K.; Lee, J.; Hilderbrand, S. A.; Weissleder, R.; Bawendi, M. G. *J. Am. Chem. Soc.* **2010**, *132*, 7838–7839.

(10) (a) Goldman, E. R.; Balighian, E. D.; Mattoussi, H.; Kuno., M. K.; Mauro, J. M.; Tran, P. T.; Anderson, G. P. *J. Am. Chem. Soc.* **2002**, *124*, 6378–6382. (b) Wu, X.; Liu, H.; Liu, J.; Haley, K. N.; Treadway, J. A.; Larson, J. P.; Ge, N.; Peale, F.; Bruchez, M. P. *Nat. Biotechnol.* **2003**, *21*, 41–46.

(11) (a) De la Fuente, J. M.; Penades, S. *Tetrahedron Asymm.* **2005**, *16*, 387–391. (b) Robinson, A.; Fang, J. M.; Chou, P. T.; Liao, K. W.; Chu., R. M.; Lee., S. J. *ChemBioChem* **2005**, *6*, 1899–1905. (c) Niikura, K.; Nishio, T.; Akita, H.; Matsuo, Y.; Kamitani, R.; Kogure, K.; Harashima, H.; Ijiro, K. *ChemBioChem* **2007**, *8*, 379–384. (d) Babu, P.; Sinha, S.; Surolia, A. *Bioconj. Chem.* **2007**, *18*, 146–151. (e) Niikura, K.; Nishio, T.; Akita, H.; Matsuo, Y.; Kamitani, R.; Kogure, K.; Harashima, H.; Ijiro, K. *ChemBioChem* **2008**, *9*, 2623–2627. (f) Yu, M.; Yang, Y.; Han, R.; Zheng, Q.; Wang, L.; Hong, Y.; Li, Z.; Sha, Y. *Langmuir* **2010**, *26*, 8534–8539.

(12) (a) Holmlin, R. E.; Chen, X.; Chapman, R. G.; Takayama, S.; Whitesides, G. M. *Langmuir* **2001**, *17*, 2841–2850. (b) Tegoulia, V. A.; Rao, W.; Kalambur, A. T.; Rabolt, J. F.; Cooper, S. L. *Langmuir* **2001**, *17*, 4396–4404. (c) Chen, S.; Zheng, J.; Li, L.; Jiang, S. *J. Am. Chem. Soc.* **2005**, *127*, 14473–14478. (d) Naruchi, K.; Nishimura, S.-I. *Angew. Chem., Int. Ed.* **2011**, *50*, 1328–1331.

(13) Nagahori, N.; Abe, M.; Nishimura, S.-I. *Biochemistry* **2009**, *48*, 583–594.

(14) Nagahori, N.; Nishimura, S.-I. *Chem. Eur, J.* **2006**, *12*, 6478–6485.

(15) (a) Bailey, R. E.; Nie, S. *J. Am. Chem. Soc.* **2003**, *125*, 7100–7106. (b) Bailey, R. E.; Strausburg, J. B.; Nie, S. A. *J. Nanosci. Nanotech.* **2004**, *4*, 569–574. (c) Jin, T.; Fujii, F.; Komai, Y.; Seki, J.; Seiyama, A.; Yoshioka, Y. *Int. J. Mol. Sci.* **2008**, *9*, 2044–2061.

(16) (a) Jin, T.; Fujii, F.; Sakata, H.; Tamura, M.; Kinjo, M. *Chem. Commun.* **2005**, 2829–2831. (b) Heuff, R. F.; Swift, J. L.; Cramb, D. T. *Phys. Chem. Chem. Phys.* **2007**, *9*, 1870–1880.

(17) Pale-Grosdemange, C.; Simon, E. S.; Prime, K. L.; Whiteside, G. M. *J. Am. Chem. Soc.* **1991**, *113*, 12–20.

(18) Kim, S.; Bawendi, M. G. *J. Am. Chem. Soc.* **2003**, *125*, 14652–14653.

(19) (a) Nishimura, S.-I.; Niikura, K.; Kurogochi, M.; Matsushita, T.; Fumoto, M.; Hinou, H.; Kamitani, R.; Nakagawa, H.; Deguchi, K.; Miura, N.; Monde, K.; Kondo, H. *Angew. Chem., Int. Ed.* **2004**, *44*, 91–96. (b) Kurogochi, M.; Amano, M.; Fumoto, M.; Takimoto, A.; Kondo, H.; Nishimura, S.-I. *Angew. Chem., Int. Ed.* **2007**, *46*, 8808–8813. (c) Miura, Y.; Hato, M.; Shinohara, Y.; Kuramoto, H.; Furukawa, J.; Kurogochi, M.; Shimaoka, H.; Tada, M.; Nakanishi, K.; Ozaki, M.; Todo, S.; Nishimura, S.-I. *Mol. Cell. Proteomics* **2008**, *7*, 370–377. (d) Furukawa, J.; Shinohara, Y.; Kuramoto, H.; Miura, Y.; Shimaoka, H.; Kurogochi, M.; Nakano, M.; Nishimura, S.-I. *Anal. Chem.* **2008**, *80*, 1094–1101. (e) Amano, M.; Yamaguchi, M.; Takegawa, Y.; Yamashita, T.; Terashima, M.; Furukawa, J.-i.; Miura, Y.; Shinohara, Y.; Iwasaki, N.; Minami, A.; Nishimura, S.-I. *Mol. Cell. Proteomics* **2010**, *9*, 523–537. (f) Kurogochi, M.; Matsushita, T.; Amano, M.; Furukawa, J.-i.; Shinohara, Y.; Aoshima, M.; Nishimura, S.-I. *Mol. Cell. Proteomics* **2010**, *9*, 2354–2368. (g) Miura, Y.; Kato, K.; Takegawa, Y.; Kurogochi, M.; Furukawa, J.-i.; Shinohara, Y.; Nagahori, N.; Amano, M.; Hinou, H.; Nishimura, S.-I. *Anal. Chem.* **2010**, *82*, 10021–10029.

(20) (a) Fumoto, M.; Hinou, H.; Matsushita, T.; Kurogochi, M.; Ohta, T.; Ito, T.; Yamada, K.; Takimoto, A.; Kondo, H.; Inazu, T.; Nishimura, S.-I. *Angew. Chem., Int. Ed.* **2005**, *44*, 2534–2537. (b) Fumoto, M.; Hinou, H.; Ohta, T.; Ito, T.; Yamada, K.; Takimoto, A.; Kondo, H.; Shimizu, H.; Inazu, T.; Nakahara, Y.; Nishimura, S.-I. *J. Am. Chem. Soc.* **2005**, *127*, 11804–11818. (c) Ohyabu, N.; Hinou, H.; Matsushita, T.; Izumi, R.; Shimizu, H.; Kawamoto, K.; Numata, Y.; Togame, H.; Takemoto, H.; Kondo, H.; Nishimura, S.-I. *J. Am. Chem. Soc.* **2009**, *131*, 17102–17109. (d) Matsushita, T.; Nagashima, I.; Fumoto, M.; Ohta, T.; Yamada, K.; Shimizu, H.; Hinou, H.; Naruchi, K.; Ito, T.; Kondo, H.; Nishimura, S.-I. *J. Am. Chem. Soc.* **2010**, *132*, 16651–16656.

(21) (a) Frangioni, J. V. *Curr. Opn. Chem. Biol.* **2003**, *7*, 626–634. (b) Lim, Y. T.; Kim, S.; Nakayama, A.; Stott, N. E.; Bawendi, M. G.; Frangioni, J. V. *Mol. Imaging* **2003**, *2*, 50–64. (c) Choi, H. S.; Ipe, B. I.; Misra, P.; Lee, J. H.; Bawendi, M. G.; Frangioni, J. V. *Nano Lett.* **2009**, *9*, 2354–2359.

(22) (a) Lunney, J.; Ashwell, G. *Proc. Natl. Acad. Sci. U.S.A.* **1976**, *73*, 341–343. (b) Stockert, R. J.; Morell, A. G.; Scheinberg, H. *Biochem. Biophys. Res. Commun.* **1976**, *68*, 988–993. (c) Kawasaki, T.; Etoh, R.; Yamashina, I. *Biochem. Biophys. Res. Commun.* **1978**, *81*, 1018–1024. (d) Prieels, J.-P.; Pizzo, S. V.; Glasgow, L. R.; Paulson, J. C. *Proc. Natl. Acad. Sci. U.S.A.* **1978**, *75*, 2215–2219. (e) Baenziger, J.; Flete, D. *Cell* **1980**, *22*, 611–620. (f) Ashwell, G.; Harford, J. *Annu. Rev. Biochem.* **1982**, *51*, 531–554.

(23) (a) Somers, W. S.; Tang, J.; Shaaw, G. D.; Camphausen, R. T. *Cell* **2000**, *103*, 467–479. (b) Varki, A. *Proc. Natl. Acad. Sci. U.S.A.* **1994**, *91*, 7390–7397. (c) Rosen, S. D.; Bertozzi, C. R. *Curr. Opin. Cell Biol.* **1994**, *6*, 663–673. (d) Rosen, S. D. *Annu. Rev. Immunol.* **2004**, *22*, 129–156.

(24) (a) Elliot, S.; et al. *Nat. Biotechnol.* **2003**, *21*, 414–421. (b) Sato, M.; Furuike, T.; Sadamoto, R.; Fujitani, N.; Nakahara, T.; Niikura, K.; Monde, K.; Kondo, H.; Nishimura, S.-I. *J. Am. Chem. Soc.* **2004**,

126, 14013–14022. (c) Kaneko, Y.; Nimmerjahn, F.; Ravetch, J. V. *Science* **2006**, *313*, 670–673. (d) Ueda, T.; et al. *J. Am. Chem. Soc.* **2009**, *131*, 6237–6245.

(25) (a) Wanger, V.; Dullaart, A.; Bock, A.-K.; Zweck, A. *Nat. Biotechnol.* **2006**, *24*, 1211–1217. (b) Verma, A.; Uzun, O.; Hu, Y.; Hu, Y.; Han, H. S.; Watson, N.; Chen, S.; Irvine, D. J.; Stellacci, F. *Nat. Mater.* **2008**, *7*, 588–595. (c) Farokhzad, O. C.; Langer, R. *ACS Nano* **2009**, *3*, 16–20. (d) Hammond, P. T. *ACS Nano* **2011**, *5*, 681–684.